Journal of the European Ceramic Society 16 (1996) 619–626

0955-2219/96/$15.00
0955-2219(95)00183-2

Characterisation of Sol–Gel Derived Alumina–Silica Matrices For Continuous Fibre Reinforced Composites

J. Wu, M. Chen,* F. R. Jones & P. F. James

Department of Engineering Materials, University of Sheffield, Sir Robert Hadfield Building, Mappin Street, Sheffield S1 3JD, UK

(Received 20 July 1995; revised version received 29 September 1995; accepted 12 October 1995)

Abstract

Bulk gels corresponding to an oxide composition of $3Al_2O_3{\cdot}2SiO_2$, prepared from a sol with a high solids yield using submicron alumina powder and colloidal silica sol as precursors, were sintered to over 99% of theoretical density after 2 h at 1300°C. Densification occurred by viscous flow of the amorphous silica matrix containing well dispersed alumina particles. After 2 h at 1600°C almost complete crystallisation to mullite occurred. Uniform unidirectional carbon fibre reinforced composites were produced by a single stage infiltration of fibres, using the above sol, and hot-pressing either at 1300 or at 1400°C to 98 and 97% of the theoretical density respectively. The composites, with a matrix predominantly of silica glass and dispersed alumina particles, exhibited non-brittle failure with mean flexural strengths of 720 and 766 MPa for hot-pressing at 1300 and 1400°C respectively. Extensive fibre pull-out during testing indicated a relatively weak bond between the fibres and the matrix, and transmission electron microscopy revealed no evidence of chemical interactions at the interface.

Introduction

Mullite ceramics are potential matrix materials for high temperature structural composite applications because of their excellent high temperature strength and creep resistance, good chemical and thermal stability and low thermal expansion coefficient. Fabrication of mullite ceramics by traditional methods using natural minerals as starting materials with alumina additions normally requires a high processing temperature in excess of 1700°C with lengthy sintering.[1,2] However, a mullite crystallisation temperature as low as 980°C can be achieved from alkoxide precursors using the molecular scale mixing of sol–gel methods.[3,4] Generally, the materials obtained by this technique suffer high shrinkages on drying because of the low solids content of the sols. If this disadvantage could be overcome, the sol–gel route would be extremely promising for the preparation of mullite composites especially when continuous fibre is used as the reinforcement.[5] In practice, the fabrication of composites by sol–gel methods have several inherent advantages over other methods such as slurry infiltration, melt-infiltration or CVD processing.[6] The consolidation of matrix and fibre can be realised in a single infiltration stage so that there is less damage to the fibres. It is also relatively easy to achieve a uniform fibre distribution. Organic binders are not required so porosity associated with burning-off is not a problem, and green strength remains high. However the much lower processing temperatures in sol–gel processing are a key factor. In preliminary work,[7,8] a colloidal sol with high solids yield containing up to 40% solids by volume, producing dried gels of the mullite composition, $3Al_2O_3{\cdot}2Sio_2$, was reported. This was used to prepare a highly densified monolithic mullite bulk ceramic with almost complete mullitisation at 1600°C after 2 h. It was also demonstrated subsequently[9] that highly densified continuous carbon fibre reinforced mullite matrix composites could be successfully prepared by a single stage infiltration process, followed by hot-pressing. Recently, Colomban and coworkers[10] have described the effects of a zirconia interphase on the mechanical properties of continuous oxide fibre reinforced mullite matrix composites prepared by a sol–gel route. The oxide fibres were in the form of woven fabric. Achievement of a non-brittle composite was related to the absence of a chemical reaction between the zirconia interphase and the oxide fibres.

---

*Present address: Department of Materials Science and Metallurgy, University of Cambridge, UK.

In this paper, densified mullite bulk gels and hot-pressed carbon fibre alumina–silica matrix composites from the high solid yield sol are characterised by X-ray diffraction (XRD), scanning electron microscopy (SEM) and transmission electron microscopy (TEM). The densification mechanism for mullite bulk gel samples is determined. The strength and elastic properties of the composites are measured under three point bending. The fracture surfaces of the composite specimens are examined by SEM, and the interface between fibre and matrix analysed by TEM.

Experimental

Monolithic samples of the mullite composition ($3Al_2O_3{\cdot}2SiO_2$) were prepared by a sol–gel process, as described in preliminary studies,[7,8] using Ludox colloidal silica sol (Dupont AS40, 40 wt% of silica, particles of 5–50 nm in diameter) and α-alumina powder (A1000 SG, Alcoa 0·5 μm) as precursors. Briefly, the pH of the Ludox sol was adjusted from 9 to 2–3 using dilute acid (HCl 1 M). Alumina powder was dispersed in the sol to achieve a uniform mixture of the required composition, using magnetic stirring. Dilute acid was again added to reduce the pH to 5–6, so that gelation occurred in 30 min. Samples of the bulk gel (discs 30 mm in diameter and 10 mm in thickness) were slowly dried at room temperature for 48 h, followed by drying at 90°C for 48 h, and calcined at 500°C for 2 h; finally they were heated at 20°C/min to the sintering temperatures (1100–1600°C) for the required holding time of 2 h.

Unidirectional carbon fibre reinforced composites were fabricated using single stage infiltration with the above sol, which had a total solids content of 40 vol%. Grafil LXA unsized high strength carbon fibre tows (density $1{\cdot}81 \times 10^3$ kg/m^3, diameter of 8 μm, theoretical strength 4 GPa, elastic modulus of 224 GPa) were employed as the reinforcement. Fibre tows were passed through the sol and wound onto a hexagonal drum to form a 10 mm thick green prepreg sheet. After drying at 90°C, the sheet was released from the drum. The dried sheet was cut into circular discs 45 mm in diameter and hot-pressed in a graphite die surrounded by a high temperature furnace. During hot-pressing, the composite prepreg was sealed by graphite powder to protect it from oxidation and a nitrogen gas flow was used to protect the die. One composite sample was heated at 20°C/min to 1300°C and held for 1 h, under a pressure of 25 MPa. Another sample was heated at 20°C/min to 1400°C and held for 0·5 h at 17 MPa. Both samples were subsequently allowed to cool naturally to room temperature overnight. By careful control of the sol viscosity, composites with a range of fibre volume fractions (0·30–0·60) could be prepared. The composites hot-pressed at 1300 and 1400°C had volume fractions of 0·40 and 0·45 respectively.

The densities of the sintered monolithic gel, and composite samples were determined by mercury immersion. The volume fraction of fibre in the composite was accurately determined from the weight change after complete oxidative removal of the carbon fibre at 900°C overnight. After this treatment, the remaining oxide matrix was white in appearance on the outside surface and on the inside after fracture, indicating that no carbon remained. The crystalline phase development in the heat treated samples was characterised by powder X-ray diffraction (Philips 1710) using a scanning speed of 2° (2θ) /min. Microstructural analysis was carried out using a Camscan 400 SEM and Philips 400 TEM. Both fracture and polished surfaces of samples were employed in the SEM study. Thin section samples for TEM study were prepared by grinding and polishing discs of 3 mm in diameter, cut from as-prepared samples to a thickness of about 100 μm and further dimpling down to about 15–20 μm in the centre, followed by final ion beam thinning to electron transparency.

The thermal expansion coefficient of the bulk gel of the alumina–silica mixture, $3Al_2O_3{\cdot}2SiO_2$, fired at 1300°C for 2 h with a density of $3{\cdot}23 \times 10^3$ kg/m^3, was measured using a dilatometer with fused silica as a reference. The measuring specimen was cut from a sintered bulk sample, and ground and polished to the diameter of 10 mm and length of 30 mm. The thermal expansion coefficient was an average result in the temperature range of 25–700°C.

The flexural strength and elastic modulus of the composite specimen were determined by three point bend test according to British Standard Methods of Testing[11] on a Mayes Universal Tester with a loading speed of 0·2 mm/min at room temperature. Rectangular test specimens cut from the hot-pressed composite were ground and polished to a span of 30 mm with a span to thickness ratio greater than 20. The reported strength is the mean of six measurements.

Results

Figure 1 shows the densification of the as-prepared bulk samples after 2 h at firing temperatures from 1100 to 1600°C. The results represent an analysis of more extensive data than given in a previous report.[8] The green density of the bulk gels was 60% of the calculated theoretical density

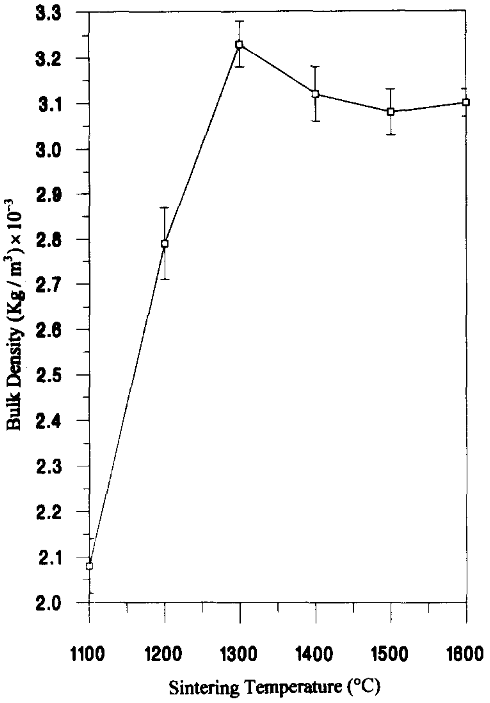

Fig. 1. Densification of the bulk gels from α-alumina powder and Ludox silica sol, corresponding to an oxide composition of $3Al_2O_3{\cdot}2SiO_2$, fired at the heating rate of 20°C/min to the sintering temperature with 2 h hold.

of $3{\cdot}25 \times 10^3$ kg/m^3 for the alumina–silica solids mixture, $3Al_2O_3{\cdot}2SiO_2$, based on the densities of $3{\cdot}98 \times 10^3$ kg/m^3)for α-alumina and $2{\cdot}22 \times 10^3$ kg/m^3 for silica glass.[12,13] Significant densification of the bulk samples began at 1100°C with substantial density increase occurring between 1200 and 1300°C. A maximum bulk density of $3{\cdot}23 \times 10^3$ kg/m^3 (over 99% of the theoretical value) was obtained at 1300°C. Sintering at higher temperatures resulted in a slightly lower bulk density of $3{\cdot}10 \times 10^3$ kg/m^3.

Figure 2 shows the XRD patterns of the as-sintered gels in the temperature range of 1200–1600°C for 2 h. The dominant crystalline phase at 1200 and 1300°C was α-alumina and no crystalline mullite was detected. The presence of a trace of cristobalite at 1200°C indicated that the amorphous colloidal silica had partially crystallised at this temperature. The extent of cristobalite formation increased after heating at 1300 and 1400°C. At around 1450°C, the crystalline mullite phase became detectable (not shown). A significant amount of mullite appeared at 1500°C at the expense of the α-Al_2O_3 and cristobalite. On firing at 1600°C, the mullite phase became dominant, with a trace of unreacted α-Al_2O_3 and cristobalite just detectable.

The high level of densification of the bulk gel is confirmed by the scanning electron micrograph shown in Fig. 3(a), where the fracture surface of a bulk sample sintered at 1300°C for 2 h, clearly demonstrates the effectiveness of the processing technique. Figure 3(b) shows the microstructure of the polished and thermal-etched (1500°C for 3 h) surface of a bulk gel which had been sintered at 1600°C for 2 h, where the fine grain structure is revealed. Based on the XRD results (Fig. 2), these grains predominantly consisted of mullite.

Figure 4 shows the transmission electron micrographs of the samples sintered at various temperatures. The submicron alumina particles were uniformly dispersed in a matrix consisting of fine colloidal silica and fine pores (diameters around 10–50 nm) at temperatures up to 900°C (Fig. 4(a)). Sintering the same gel to 1200°C resulted in a reduction in the total porosity but with significant pore coarsening to diameters around 0·1 μm (Fig. 4(b). A detailed study revealed that the pores were interconnected to form channels around dispersed alumina particles. At this temperature, as shown in Fig. 1, partial sintering had occurred, with a corresponding density of $2{\cdot}79 \times 10^3$ kg/m^3, compared with $2{\cdot}0 \times 10^3$ kg/m^3 for the unsintered gel. Almost complete densification was achieved after

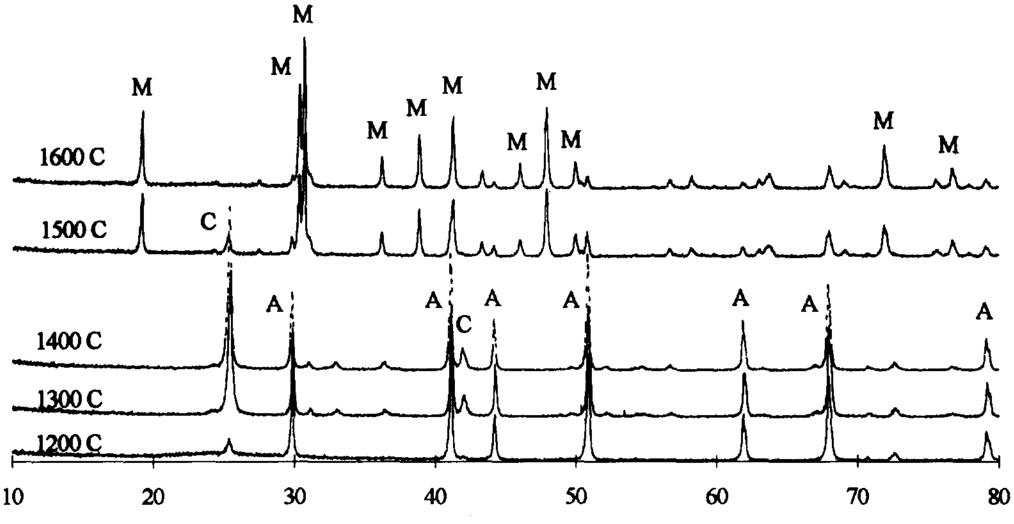

Fig. 2. XRD results of the bulk gels from α-alumina powder and Ludox silica sol, with the composition, $3Al_2O_3{\cdot}2SiO_2$, fired at the heating rate of 20°C/min to heating temperatures in the range of 1200–1600°C with 2 h hold.

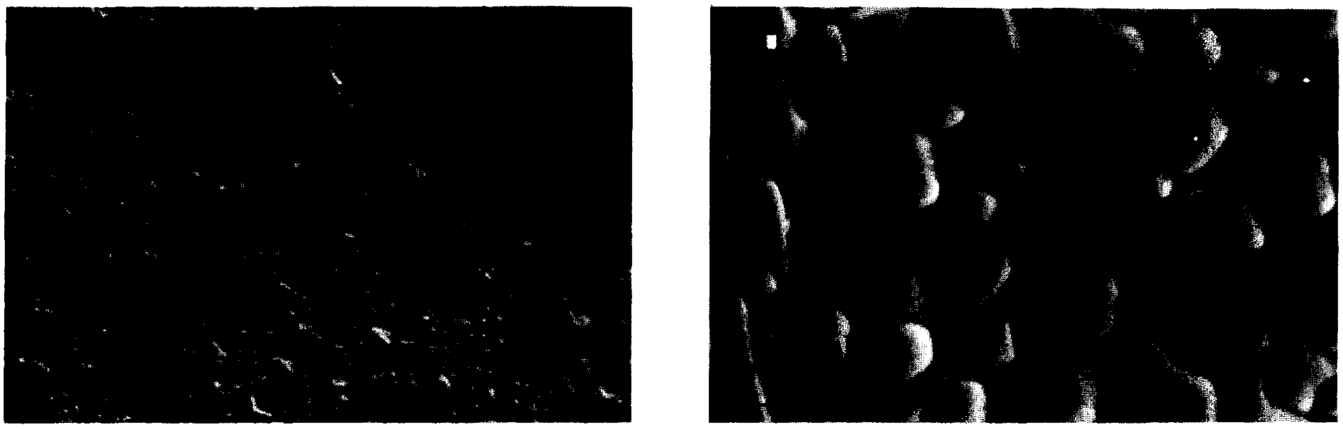

(a) (b)

Fig. 3. SEM of a unetched fracture surface (a), and a polished and thermally etched surface (b) of the bulk gels from α-alumina powder and Ludox silica sol, with the composition, $3Al_2O_3{\cdot}2SiO_2$, fired at 1300 and 1600°C for 2 h respectively.The bars denote 3 μm for (a) and 1 μm for (b).

2 h at 1300°C, as shown by the almost pore-free microstructure (Fig. 4(c)). The fine alumina particles were individually dispersed in the already highly densified silica matrix. No agglomerates of alumina particles, which could have resulted in sintering voids were observed. From TEM and selected area electron diffraction, the silica matrix was predominantly amorphous but did occasion-

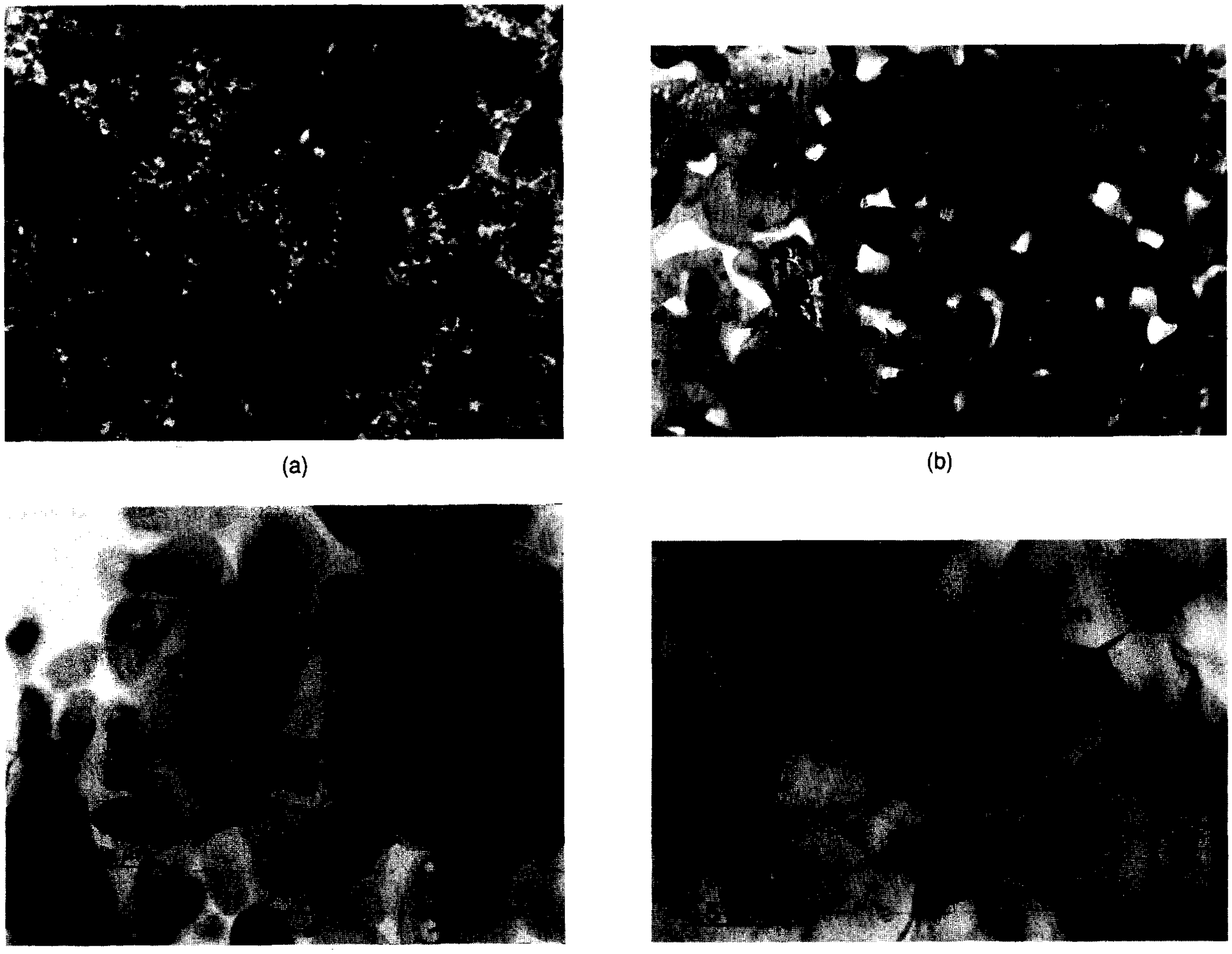

(a) (b) (c) (d)

Fig. 4. TEM of the bulk samples from α-alumina powder and Ludox silica sol, with the composition, $3Al_2O_3{\cdot}2SiO_2$, fired at 900°C (a), 1200°C (b), 1300°C (c) and 1600°C (d) for 2 h respectively. The bars denote 0·5 μm for (a), 0·3 μm for (b), 0·5 μm for (c) and 0·5 μm for (d), and a, s, p and m denote α-alumina particle, silica (glass), pore and mullite grain respectively. In Fig. 4(d), a small region of unreacted alumina is arrowed.

ally contain some fine crystals, probably cristobalite since they were much finer than the alumina particles. The presence of cristobalite was also indicated by XRD. After firing at 1600°C for 2 h a uniform microstructure of crystal grains with diameters around 1 μm was observed by TEM (Fig. 4(d)), confirming SEM observations (Fig. 3(b)). XRD shows a predominance of crystalline mullite with traces of alumina and cristobalite, suggesting that most of the alumina particles had reacted with the surrounding silica matrix to form mullite, although small spherical particles within the mullite grains were occasionally visible by TEM (Fig. 4(a)), which probably represent small regions of unreacted crystalline alumina. Small regions at mullite triple grain junctions, probably of unreacted silica, were also occasionally observed.

A few small pores were also observed by TEM within the mullite microstructure, showing that the sample had not completely densified after heat treatment at 1600°C. Some of the pores may have originated not in sintering but in the precursor α-alumina particles themselves. From Fig. 1 the bulk density after 2 h at 1600°C was $3{\cdot}1 \times 10^3$ kg/m^3, approximately 98% of the theoretical density for mullite ($3{\cdot}17 \times$ kg/m^3).

Figure 5(a) shows a polished cross-section (perpendicular to the fibre direction) of the composite (V_f=0·40, hot-pressed at 1300°C for 1 h), which demonstrates the uniform distribution of carbon fibres within the matrix. The matrix was composed of unreacted alumina particles in a silica matrix (mainly silica glass). Figure 5(b) shows a polished cross-section parallel to the fibre direction. Regularly spaced transverse microcracks (average spacing 103 μm) are clearly observed running perpendicular to the fibre direction. These are probably caused by the difference in thermal expansion coefficients between the alumina–silica matrix and carbon fibre. The overall average thermal expansion coefficient of the matrix is around $4{\cdot}1 \times 10^{-6}$ K^{-1} based on measurement carried out on the bulk gel sample sintered at 1300°C for 2 h. This value compares with a value of approximately zero for the carbon fibre, producing a large thermal mismatch on cooling from the processing temperature, and resulting in transverse crack formation. Further detailed examination of the microstructure of the composite by SEM revealed no additional cracks or voids in the matrix, in good agreement with the density measurements of approximately 98% of the calculated theoretical density ($2{\cdot}67 \times 10^3$ kg/m^3) for the composite.

The microstructure of the composite hot-pressed at 1400°C were very similar to that of the composite hot-pressed at 1300°C. Properties of the composites are presented in Table 1, which shows the mean values, determined by three point bending, where V_f is the fibre volume fraction σ the flexural strength, E the elastic modulus, and ρ/ρ_0 the ratio of density to the calculated theoretical density. σ_0 and E_0 are the calculated theoretical strength and elastic modulus of the composite by the rule of mixtures assuming that there is no contribution from the matrix (see Discussion). Also included is the fracture surface energy, W, for the 1300°C composite calculated from the areas under the stress–strain curves.

(a)

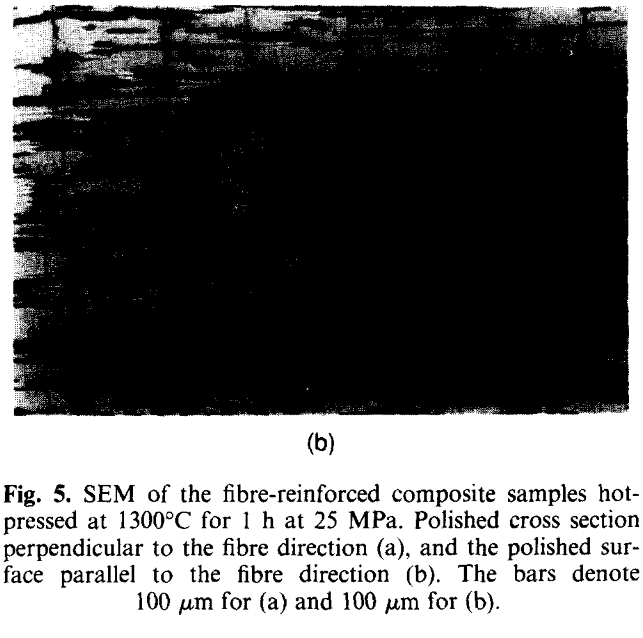

(b)

Fig. 5. SEM of the fibre-reinforced composite samples hot-pressed at 1300°C for 1 h at 25 MPa. Polished cross section perpendicular to the fibre direction (a), and the polished surface parallel to the fibre direction (b). The bars denote 100 μm for (a) and 100 μm for (b).

The hot-pressing conditions yielded composites with an average flexural strength and an average elastic modulus of 720 MPa and 107 GPa respectively at 1300°C and 766 MPa and 80 GPa respectively at 1400°C. All tested specimens showed non-brittle fracture behaviour. Figure 6 shows a typical loading stress against deflection curve for the composite under three point bending. Extensive fibre pull-out was observed in the fracture surface on the tensile side of the specimens, as shown in Fig. 7(a), suggesting a weak fibre/matrix interface. Both SEM and TEM (Fig. 7(b)) studies

Table 1. The properties of the composites

Hot-pressing condition	*1300°C, 25 MPa, 1 h*	*1400°C, 17 MPa, 0·5 h*
V_f	0·4	0·45
ρ/ρ_0	0·98	0·97
σ(MPa)	720±156	766±150
E(GPa)	107±33	80±15
W(kJ/m^3)	318±69	—
σ_0 (GPa)	1·6	1·8
E_0 (GPa)	90	100

± values are standard deviations

suggested no obvious reaction or evidence of strong bonding at the interface between the carbon fibre and the matrix.

Discussion

The bulk gel samples demonstrated high sinterability and a relatively low sintering temperature, almost full densification being achieved at 1300°C after 2 h. Similar results have been obtained previously on compacts of α-alumina particles coated with amorphous silica derived from TEOS, in which the enhanced densification was attributed to transient viscous sintering.[14] In the present case, TEM of the gel heated at 900°C shows that the alumina particles were individually dispersed in a porous silica glass matrix. Density measurement and TEM observation also indicate that during the densification process, fine pores in the silica matrix gradually collapsed and dense silica regions were formed. Moreover, the reduction in total porosity was accompanied by formation of larger interconnected pores, while the morphology of the submicron alumina particles remained unchanged. The densification mechanism consisted of viscous flow of the amorphous silica matrix, followed by rearrangement of the dispersed solid alumina particles. It is clear that at 1300°C the viscosity of the silica glass is low enough to allow collapse of remaining pores and mass transport around the alumina particles. The solid alumina particles are expected to reduce the densification rate by retarding viscous flow. However, TEM observations show that the alumina particles are well separated and do not form an interlocking network,

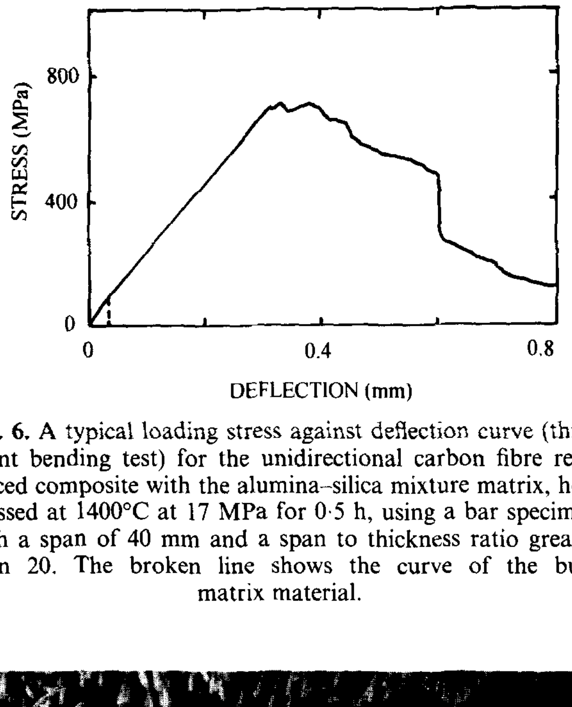

Fig. 6. A typical loading stress against deflection curve (three point bending test) for the unidirectional carbon fibre reinforced composite with the alumina–silica mixture matrix, hot-pressed at 1400°C at 17 MPa for 0·5 h, using a bar specimen with a span of 40 mm and a span to thickness ratio greater than 20. The broken line shows the curve of the bulk matrix material.

(a) (b)

Fig. 7(a) an SEM of the fracture surface of a composite specimen after three point bend test; (b) a TEM of an interface of the composite. The bars denote 100 μm for (a) and 0·1 μm for (b). The unidirectional carbon fibre reinforced composite with the alumina–silica mixture matrix was consolidated by hot-pressing at 1300°C for 1 h at 25 MPa.

which probably explains why few residual pores were retained in the microstructure prior to crystallisation of the silica to cristobalite, and the reaction of the silica and alumina to form mullite. Mullitisation started at temperatures above 1400°C following complete densification, because of the reaction of submicron alumina particles with the silica phase. The presence of occasional unreacted alumina surrounded by the mullite and the pockets of residual silica at mullite triple grain junctions in the sample fired at 1600°C is thought to be caused by the slow diffusion rate across the mullite matrix by the end of the mullitisation.

The gradual decrease in bulk density with firing temperatures above 1300°C was noted elsewhere[7,8] and was attributed mainly to the density change caused by mullitisation, although enhanced formation of cristobalite at the higher firing temperatures, which inhibited the densification, may have been partly responsible.[8]

The matrix in the present composite samples was the alumina–silica mixture which was not converted into crystalline mullite at the processing temperatures of 1300 and 1400°C. Mullite matrix composites can be formed by hot-pressing at higher temperatures, which has been reported elsewhere[9] and the properties of these composites will be discussed in detail in a later publication. The flexural strength and elastic modulus of the composites are somewhat lower than those theoretically predicted by the rule of mixtures, according to the following equations:

$$\sigma_c = \sigma_m V_m + \sigma_f V_f \qquad (1)$$

$$E_c = E_m V_m + E_f V_f \qquad (2)$$

Here the subscripts c, m and f refer to the composite, matrix and fibres respectively. The observation of thermally induced transverse cracks in the matrix indicates that the matrix strength is low and that the first term in eqn (1) may be neglected. However, the experimental strengths remain much lower than the theoretical values (Table 1) which may be explained by some degradation in the strength of the carbon fibres during hot-pressing. On the other hand, the predicted and measured elastic moduli of the composite are in a reasonable agreement, also neglecting the effect of the matrix in eqn (2).

The non-brittle-mode failure of the composite was clearly shown by the loading stress against deflection curve (Fig. 6), and the extensive fibre pull-out (Fig. 7(a)) on the tensile side in the fracture surface after the three point bend test. This suggests a comparatively weak interfacial bond between the fibres and the matrix, which is supported by no apparent evidence of chemical interactions at the interface from TEM observation Fig. 7(b).

Conclusions

Bulk gels corresponding to an oxide (mullite) composition, $3Al_2O_3{\cdot}2SiO_2$, were fabricated using submicron α-alumina powder and colloidal silica sol as precursors and characterised after heat-treatment by density measurement, XRD, SEM and TEM. Bulk gels were sintered to almost full density ($3{\cdot}23 \times 10^3$ kg/m^3, over 99% of the theoretical value of $3{\cdot}25 \times 10^3$ kg/m^3) at the relatively low temperature of 1300°C. From TEM and other observations, the densification mechanism clearly consisted of viscous flow of the amorphous silica matrix and rearrangement of well dispersed solid alumina particles, which did not form an interlocking network.

X-ray diffraction revealed increasing amounts of cristobalite for heat treatments above 1200°C. Mullite was detected around 1450°C and was dominant after 2 h at 1600°C, with a trace of unreacted alumina and cristobalite just detectable. After 2 h at 1600°C an uniform microstructure of mullite grains with diameters around 1 μm was obtained. The samples remained almost fully densified after mullitisation at 1600°C ($3{\cdot}10 \times 10^3$ kg/m^3 corresponding to approximately 98% of the theoretical density of $3{\cdot}17 \times 10^3$ kg/m^3 for mullite).

A sol–gel route for processing continuous unidirectional fibre composites was developed involving a simple single stage infiltration process followed by hot-pressing and avoiding the multiple impregnation often required in the use of sol–gel methods.[15]

Efficient fibre infiltration with reduced processing shrinkages was achieved by using the low viscosity sol with a high solid yield, prepared from submicron alumina powder and colloidal silica sol as precursors. The method also gave a uniform distribution of fibres and enabled the volume fraction of fibres to be adjusted. Densification of 98% to a matrix consisting mainly of alumina particles and silica glass was achieved by hot-pressing at the relatively low temperature of 1300°C.

The composites exhibited non-brittle fracture with a mean flexural strength, under three point bending, of 720 MPa for hot-pressing at 1300°C and 766 MPa for hot-pressing at 1400°C, Extensive fibre pull-out was observed after testing, indicating a relatively weak bond between the fibres and the matrix. This was supported by TEM observations which revealed a clear defined fibre/matrix interface and no evidence of chemical interactions.

Acknowledgements

Thanks are due to the Chinese Government and the British Council for financial support (J. Wu) and to the Dupont company for the supply of Ludox colloidal silica sol.

References

1. Sacks, M. D. Lee, H. W. & Pask, J. A., A review of powder preparation methods and densification procedures for fabricating high density mullite, *Ceram. Trans. Vol. 6. Mullite and Mullite Matrix Composites*, ed. S. Somiya, R. F. Davis & J. A. Pask, 1990, pp. 167–207.
2. Sing, R. N. & Gaddipati, A. R., Mechanical properties of a uniaxially reinforced mullite–silicon carbide composite. *J. Am. Ceram. Soc.*, **71** (1988) C100.
3. Yoldas, B. E., Mullite formation from aluminium and silicon alkoxides, *Ceram. Trans. Vol. 6. Mullite and Mullite Matrix Composites*, ed. S. Somiya, R. F. Davis & J. A. Pask, 1990, pp. 255–62.
4. Taylor, A. & Holland, D., The chemical synthesis and crystallisation sequence of mullite, *J. Non-Crystalline Solids*, **152** (1993) 1–17.
5. Chen, M., James, P. F., Jones, F. R. & Bailey, J. E., Alumina ceramic matrices for fibre composites prepared by modified sol–gel processing, *Inst. Phys. Conf.*, Ser No. 111, 1990, pp. 227–37.
6. Qi, D. & Pantano, C. G., Sol–gel processing of carbon-fiber-reinforced glass matrix composites. In *3rd Int. Conf. on Ultrastructure Processing of Ceramics, Glasses and Composites*, ed. J. D. Mackenzie & D. R. Ulrich. J. Wiley & Sons, NY 1987, pp. 635–49.
7. James, P. F., Wu, J., Chen, M. & Jones, F. R., Preparation of mullite using transient viscous sintering of alumina with sol–gel derived silica, presented at Conference on Advances in Amorphous State Chemistry, Dec. 1992, London (Society of Glass Technology & Royal Society of Chemistry), *Topical issues in Glass*, Vol. 1, April 1993, p. 77.
8. Wu, J., Chen, M., Jones, F. R. & James, P. F., Mullite and alumina–silica matrices for composites by modified sol–gel processing. *J. Non-Crystalline Solids*, **162** (1993) 197–200.
9. Wu, J., Jones, F. R. & James, P. F., Mullite matrix fibre reinforced composites by sol–gel processing, presented in 96th Am. Ceram. Soc. Annual Meeting, April 1994, Indianapolis, USA; *Ceram. Trans. Vol. 46: Advances in Ceramic Matrix Composites*, II, 1995, pp. 177–87.
10. Mouchon, E. & Colomban, Ph., Oxide ceramic matrix/oxide fibre woven fabric composites exhibiting dissipative fracture behaviour. *Composites*, **26** (1995), 175–82.
11. *British Standard Methods of Testing, Method 1005*, Determination of flexural properties–three point method, (British Standards Institution) BS 2782; Part 10; Method 1005; 1977, EN63.
12. Wang, J. G. Ponton, C. B. & Marquis, P. M., Effect of green density on crystallization and mullitisation in the transiently sintered mullite. *J. Am. Ceram. Soc.* **75** (1992) 3457–61.
13. Sosman, R. B., The Properties of Silica, *A. C. S. Monograph Series*, No. 37, New York: Chemical Catalog Co., 1927, p. 289.
14. Sacks, M. D., Bozkurt, N. & Scheiffele, G. W., Fabrication of mullite-matrix composites by transient viscous sintering of composite powders. *J. Am. Ceram. Soc.*, **74** (1991) 2428–37.
15. Sheppard, L. M., Enhancing performance of ceramic composites, *Am. Ceram. Soc. Bull.*, **71** (1992) 617.